Surface Chemistry

DOI: 10.1002/anie.200800883

Selenium as a Key Element for Highly Ordered Aromatic Self-Assembled Monolayers**

*Asif Bashir, Daniel Käfer, Jan Müller, Christof Wöll, Andreas Terfort, and Gregor Witte**

Driven by research in the emerging field of organic electronics, self-assembled monolayers (SAMs) of aromatic molecules have attracted pronounced interest because they allow detailed studies of charge-transport processes across metal–organic interfaces,[1] or have been used as contact primers to improve the properties of metal electrodes.[2–5] To make the step from being merely model systems to use in applications requires not only local order in these systems,[1,6] but also the possibility to obtain surface layers with long-range order by a rational approach. In particular, heterogeneities, which might dominate the electronic behavior, must be avoided. Therefore, a precise control of the molecular ordering and the defect density in these ultrathin organic layers is of key importance and requires a detailed microscopic understanding of both the molecule–substrate interactions and the intermolecular interactions, with the latter being particular strong for SAMs with aromatic backbones.

Among the aromatic SAMs, oligophenylenethiols in particular have been studied extensively because they are commonly considered as a model system. It has been demonstrated that their long-range ordering can be significantly improved by adding a flexible aliphatic spacer chain between the anchoring unit and the aromatic moiety.[7,8] Since the insertion of such insulating spacers significantly hampers the charge transport between the aromatic moiety and a metal substrate,[9] this strategy, however, is not a suitable approach for applications in organic or molecular electronics. Moreover, it has been shown that the inter-ring torsion between the individual phenyl units provides an additional conformational degree of freedom which also effects the packing density in such films.[10] On the other hand, in view of the successful use of acenes, such as pentacene, for electronic-device applications,[11] acenethiols constitute a promising class of SAMs to be used as injection layers. While the band gap ΔE (or HOMO–LUMO separation) of acenes decreases with increasing number of aromatic rings their solubility also decreases significantly which limits the number of available and usable acenethiols. In case of anthracene-2-thiol (AntS) the band gap amounts to $\Delta E = 3.45$ eV which is already distinctly smaller than the corresponding band gap for oligophenylene-based SAMs ($\Delta E = 4.3$–4.5 eV, see also the Supporting Information). Note, that the band gap for oligophenylene-based SAMs is almost independent of the number of phenyl units because they are separated by C–C single bonds, a feature which means that these molecules are only partly conjugated. Our previous study has shown that although AntS SAMs have excellent electronic properties, their structural quality is limited to only short-range ordering.[12] The reason for the lack of long-range order could be traced back to a misfit between the arrangement of aromatic backbones, which have a tendency to try and pack in a similar fashion to that in the bulk anthracene, and to the restrictions on intermolecular distances in a SAM imposed by the supporting Au(111) lattice. The resulting stress in the SAM is released by introducing a high density of defects, such as domain boundaries, stacking faults, or point defects, which hampers a long-range ordering.

Herein, we have analyzed a different approach to improve the structural quality of fully conjugated aromatic SAMs without introducing any spacer groups or other changes in the molecular structure. We demonstrate that replacing the sulfur anchor atom by selenium[13] can distinctly reduce the stress in aromatic SAMs, leading to a significant improvement of structural quality. In addition, the selenium anchoring is expected to provide better electronic coupling to gold than that obtained with sulfur.[14,15] While the usability of selenolates as alternative anchoring units for SAMs has been demonstrated before[16,17] their ability to improve the film ordering as well as the underlying mechanism had not been identified.

To avoid the formation of insoluble aromatic diselenides and a possible oxidation of selenium, an acetate protection group was used to enable the preparation of monolayer films by immersion (for synthesis and experimental details see the Supporting Information). Note, that the stabilization of an intermediate, flat-lying phase that was observed for acetate-protected aliphatic organothiols[18] was not observed for the present systems, most likely a result of the reduced flexibility of the aromatic (acene) backbone. Figure 1 a,c) shows typical STM micrographs recorded for a monolayer of anthracene-2-selenolate (AntSe) demonstrating the presence of long-range ordered SAMs. The data reveal characteristic stripes of closely packed molecules along the $\langle 11\bar{2} \rangle$ azimuth directions of the Au(111) substrate. This arrangement is rather robust and is not disturbed by point defects thus leading to extended domains with lateral dimensions of more than 50 nm. A

[*] A. Bashir, D. Käfer, Prof. C. Wöll, Priv.-Doz. Dr. G. Witte
Lehrstuhl für Physikalische Chemie I, Ruhr-Universität Bochum
44780 Bochum (Germany)
Fax: (+49) 234-321-4182
E-mail: witte@pc.ruhr-uni-bochum.de
Homepage: http://www.pc.rub.de

J. Müller, Prof. A. Terfort
Fachbereich Chemie, Philipps-Universität Marburg
35032 Marburg (Germany)

[**] This work was funded by the DFG (focus program OFET) and supported by a grant from the Dr. Otto Röhm Gedächtnisstiftung (A.T.) and the Studienstiftung des Deutschen Volkes (D.K.).

Supporting information for this article is available on the WWW under http://www.angewandte.org or from the author.

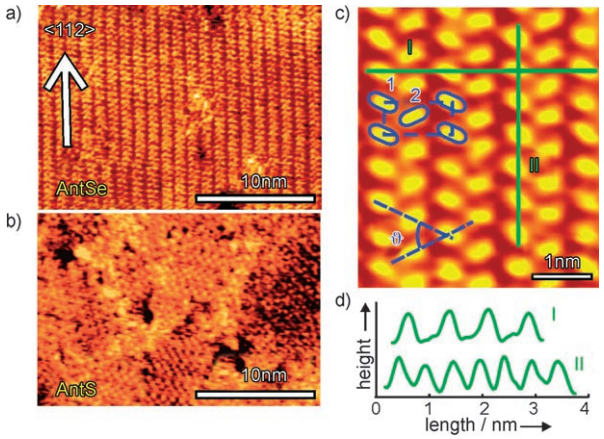

Figure 1. STM data ($U_t = -200$ mV and $I_t = 150$ pA) obtained for AntSe SAMs on Au(111): a) View of a typical single domain of AntSe on Au(111), b) comparison with STM data of the previously studied AntS SAM.[12] c) High-resolution data reveal the herringbone packing of the molecules, d) line profiles from (c) used to determine the cell parameters.

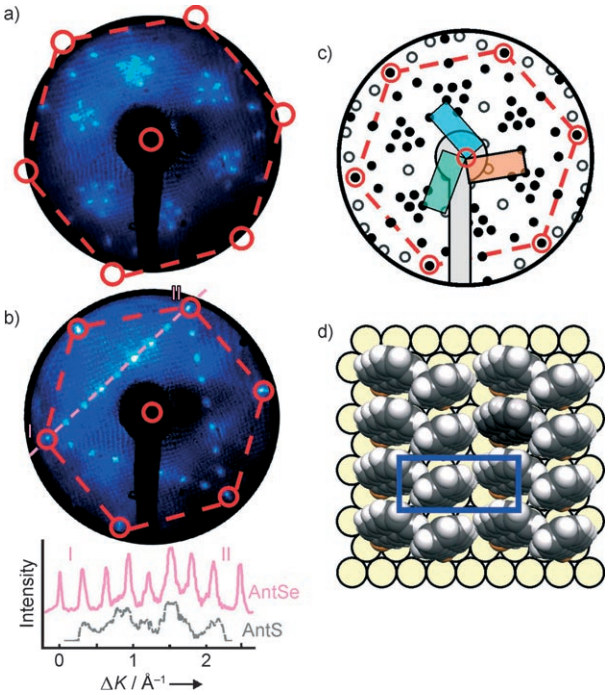

Figure 2. The measured LEED patterns a) $E = 75$ eV and b) $E = 99$ eV. c) The reciprocal lattice of a $(\sqrt{3}\times4)$*rect* structure including rotational domains. The line scan in (b) shows the presence of narrow diffraction peaks while closely spaced diffraction spots could not be resolved for AntS SAMs (dashed line).[12] The dashed hexagons in (c) represent the first-order diffraction pattern of a clean Au(111) substrate. d) A structure model of the AntSe SAM.

comparison with micrographs taken for the corresponding thiolate-anchored AntS SAMs (see Figure 1b) directly demonstrates the superior structural quality of the AntSe SAMs. Interestingly, in the AntSe SAMs no vacancy depressions or ad-islands at the gold surface (also referred to as etch-pits) are formed. In contrast, these features are found in AntS SAMs and many other thiol-based SAMs and are attributed to release of stress from the gold surface.[19] High-resolution STM micrographs (see Figure 1c) clearly reveal a characteristic herringbone arrangement of neighboring molecules forming an angle of $\vartheta = 48 \pm 3°$. To date, this packing motive has only been assumed for monolayers of upright, aromatic molecules and this is the first time it has been seen directly. It closely resembles the packing of anthracene molecules adopted in their crystalline bulk phase, which has a layered structure consisting of (001) planes with upstanding molecules forming a characteristic face-on-edge herringbone arrangement (50°).[20] In the present case, the unit-cell dimensions derived from STM measurements would allow for various commensurate superstructures.

Regarding the structural analysis of molecular layers by STM we would like to emphasize that in the absence of intrinsic markers, such as substrate atoms, a precise determination of the unit cell of molecular superstructures is usually hampered by thermal drift and/or piezo creep which typically limits the absolute accuracy of lateral dimensions by about 5–10%. To ascertain the true superstructure and to rule out the presence of an incommensurate superstructure, low-energy electron diffraction (LEED) measurements were carried out. By using a low-current micro-channel plate (MCP) LEED system, possible e-beam damage of the SAM can be safely excluded. Note that some diffraction spots reveal only low intensities as a result of out-of-phase conditions (Figure 2a,b) but can be made visible by increasing the incident beam energy.

From the position of all the observed diffraction spots relative to the first-order diffraction pattern of the gold substrate (hexagon in Figure 2a–c) the film structure can be unambiguously identified as a commensurate $(\sqrt{3}\times4)$*rect* phase. The pronounced long-range ordering of the AntSe SAMs is further indicated by the sharpness of the diffraction spots (line scan in Figure 2b) which could not be resolved for AntS SAMs (the dashed line in Figure 2b). Using the precise unit-cell dimensions of 11.54×5.0 Å derived from diffraction and considering the presence of two molecules per unit cell (see Figure 1c) this yields a molecular area of 28.8 Å^2 which is similar to the molecular packing adopted in the (001) planes of anthracene crystals (25.6 Å^2).[20]

Additional information about the molecular orientation was derived from near-edge X-ray absorption (NEXAFS) measurements. By analyzing the linear dichroism of the π* resonances, a characteristic signature of the aromatic moiety, their tilt angle ϕ relative to the surface normal can be determined (see the Supporting Information). Although this analysis is generally complicated by the presence of differently arranged molecules within the unit cell, resulting in only average orientations, in case of a herringbone arrangement the individual molecular tilt angle can be determined.[12] Using the herringbone angle obtained independently from STM data this yields a tilt of the aromatic moiety of $\phi = 33°$ which parallels the situation in anthracene crystals where molecules are tilted by 34.8° relative to the normal of the (001)-planes. A comparison of the microstructures obtained for AntS SAMs and AntSe SAMs reveals a close analogy and bears further resemblance to the molecular arrangement in

anthracene crystals which demonstrates that the structure of these acene-based SAMs is essentially governed by the aromatic moieties. Regarding the long-range ordering of both SAMs, however, significant differences were found (Figure 1a,b). Especially the absence of etch pits in case of AntSe SAMs suggests that the selenolates cope differently with the misfit to the gold lattice thus indicating the key importance of the anchoring group. We note that a moderate ordering was previously observed for SAMs of benzeneselenol (BSe) whereas the corresponding benzenethiol (BS) only forms rather disordered films.[21] In that case, however, no diffraction pattern could be observed and the real cause of the enhanced ordering was masked by the presence of very different molecular adsorption geometries adopted in both SAMs. For example BS only forms a rather loosely packed monolayer where molecules are downward tilted which enables an additional ring–substrate interaction.[21]

Additional information about the substrate interaction of both anchoring units was derived from thermal-desorption measurements (see Supporting Information). These showed only one distinct desorption peak for AntSe SAMs which indicates a single adsorption site. In contrast two different adsorption peaks were obtained for AntS SAMs which suggests the presence of two non-equivalent adsorption sites.[12] Considering further the different covalent radius of the anchoring atoms (Se 1.16 Å, S 1.02 Å) a longer bond length is expected for the selenol–gold interaction which is in agreement with recent calculations.[22] Since the intermolecular interaction between the aromatic moieties in AntSe SAMs and AntS SAMs is identical and the rigidness of both molecules excludes further any conformational changes (which can occur in case of oligophenylenes) the differences obtained in the long range ordering can be rationalized by differences in the lateral corrugation of the substrate interaction potential. Owing to the longer bond length, a smaller corrugation is seen by the selenolate which implies that a (small) lateral displacement of the selenolate from the preferred adsorption site requires less energy than for a thiolate. In this way the AntSe SAM can compensate the misfit to the substrate lattice and thus avoid a build-up of stress within the film. The underlying mechanism parallels the situation observed for the adsorption of (sub)monolayer films of alkali metals on metal surfaces. As the substrate–alkali-metal bond length increases with increasing alkali-metal size, a decrease of the lateral corrugation of the substrate holding potential is expected and could be demonstrated by measuring the frustrated translational mode parallel to the surface.[23] Moreover, this phenomenon explains the formation of quasi-epitaxial layers with hexagonal symmetry on a Cu(100) substrate for large alkali-metals whereas the small alkali metals adopt a monolayer structure with a twofold symmetry imposed by the substrate.

Herein we highlight the key importance of a microscopic understanding of molecular film formation and demonstrate that selenolate-anchoring provides an promising route to prepare highly ordered SAMs of rigid and fully conjugated aromatic molecules which are of particular interest for organic electronic applications.

Received: February 23, 2008
Published online: June 2, 2008

Keywords: electron diffraction · scanning probe microscopy · selenolate · self-assembled monolayer · surface chemistry

[1] J. M. Tour, *Acc. Chem. Res.* **2000**, *33*, 791.
[2] D. J. Gundlach, L. L. Jia, T. N. Jackson, *IEEE Electron Device Lett.* **2001**, *22*, 571.
[3] G. S. Tulevski, Q. Miao, A. Afzali, T. O. Graham, C. R. Kagan, C. Nuckolls, *J. Am. Chem. Soc.* **2006**, *128*, 1788.
[4] C. Bock, D. V. Pham, U. Kunze, D. Käfer, G. Witte, Ch. Wöll, *J. Appl. Phys.* **2006**, *100*, 114517.
[5] C. Bock, D. V. Pham, U. Kunze, D. Käfer, G. Witte, A. Terfort, *Appl. Phys. Lett.* **2007**, *91*, 052110.
[6] J. M. Seminario, *Nat. Mater.* **2005**, *4*, 111.
[7] P. Cyganik, M. Buck, W. Azzam, C. Wöll, *J. Phys. Chem. B* **2004**, *108*, 4989.
[8] P. Cyganik, M. Buck, T. Strunskus, A. Shaporenko, J. D. E. T. Wilton-Ely, M. Zharnikov, C. Wöll, *J. Am. Chem. Soc.* **2006**, *128*, 13868.
[9] L. Venkataraman, J. E. Klare, C. Nuckolls, M. S. Hybertsen, M. L. Steigerwald, *Nature* **2006**, *442*, 904.
[10] G. Heimel, L. Romaner, J. L. Bredas, E. Zojer, *Langmuir* **2008**, *24*, 474.
[11] J. E. Anthony, *Angew. Chem.* **2008**, *120*, 460; *Angew. Chem. Int. Ed.* **2008**, *47*, 452.
[12] D. Käfer, G. Witte, P. Cyganik, A. Terfort, C. Wöll, *J. Am. Chem. Soc.* **2006**, *128*, 1723.
[13] J. Müller, A. Terfort, *Inorg. Chim. Acta* **2006**, *359*, 4821.
[14] S. N. Yaliraki, M. Kemp, M. A. Ratner, *J. Am. Chem. Soc.* **1999**, *121*, 3428.
[15] L. Patrone, S. Palacin, J. Charlier, F. Armand, J. P. Bourgoin, H. Tang, S. Gauthier, *Phys. Rev. Lett.* **2003**, *91*, 096802.
[16] M. H. Dishner, J. C. Hemminger, F. J. Feher, *Langmuir* **1997**, *13*, 4788.
[17] J. D. Monnell, J. J. Stapleton, S. M. Dirk, W. A. Reinerth, J. M. Tour, D. L. Allara, P. S. Weiss, *J. Phys. Chem. B* **2005**, *109*, 20343.
[18] M. G. Badin, A. Bashir, S. Krakert, T. Strunskus, A. Terfort, C. Wöll, *Angew. Chem.* **2007**, *119*, 3837; *Angew. Chem. Int. Ed.* **2007**, *46*, 3762.
[19] G. Yang, G.-Y. Liu, *J. Phys. Chem. B* **2003**, *107*, 8746.
[20] C. Pratt, J. D. Brock, W. Dunitz, *Acta Crystallogr. Sect. B* **1990**, *46*, 795.
[21] D. Käfer, A. Bashir, G. Witte, *J. Phys. Chem. C* **2007**, *111*, 10546.
[22] J. M. Standard, B. W. Gregory, B. K. Clark, *THEOCHEM* **2007**, *803*, 103.
[23] P. Senet, J. P. Toennies, G. Witte, *Chem. Phys. Lett.* **1999**, *299*, 389.

